

Evaluation of metal artefact reduction in cone-beam computed tomography images of different dental materials

Polyane Mazucatto Queiroz¹ · Matheus Lima Oliveira¹ · Francisco Carlos Groppo² · Francisco Haiter-Neto¹ · Deborah Queiroz Freitas¹

Received: 7 September 2016 / Accepted: 15 May 2017 / Published online: 23 May 2017
© Springer-Verlag Berlin Heidelberg 2017

Abstract

Objective The aim of this study is to evaluate the efficacy of metal artefact reduction (MAR) in different dental materials with Picasso Trio cone-beam computed tomography (CBCT) scanner.

Materials and methods Three imaging phantoms were custom-made of acrylic resin. Each phantom presented three cylinders of the same material: dental amalgam alloy, gutta-percha or aluminium-copper alloy. CBCT scans were performed on Picasso Trio unit with and without MAR, and artefact expression (standard deviation of grey values) was obtained and compared by Kruskal-Wallis and Student-Newman-Keuls (post hoc) ($\alpha = 0.05$).

Results Significant reduction of artefact expression ($p < 0.05$) was observed with MAR on areas around dental alloys. No significant difference ($p > 0.05$) was observed with or without MAR when gutta-percha was scanned.

Conclusion MAR was effective in reducing artefacts arising from dental alloys on CBCT images.

Clinical relevance Dental materials of high atomic number and density are widely used in dentistry and can produce artefact that compromise CBCT image. The present study demonstrated that metal artefact reduction algorithm is an effective tool to improve image quality.

Keywords Cone-beam computed tomography · Artefacts · Dental materials · Photon absorptiometry · Densitometry

Introduction

Cone-beam computed tomography (CBCT) is an imaging modality with numerous applications and increasing acceptance in dentistry. The possibility of having an accurate three-dimensional treatment planning has brought important benefits to some dental specialties, such as dental implantology, orthodontics and oral and maxillofacial surgery [1, 2]. Most of the current CBCT units are capable of producing high-resolution images that precisely depict fine anatomical structures.

In CBCT, the interaction of the polyenergetic X-ray beam with dental materials of high density and atomic number, e.g. dental amalgam alloy, dental implant, metallic post, gutta-percha and orthodontic appliances, induces an error in the recorded data that leads to distortions unrelated to the subject studied and is known as image artefact [3, 4]. The formation of CBCT image artefact may compromise the image quality [3, 5, 6] and increase in the interpretation time by obscuring anatomical structures in the region of interest, reduce the diagnostic accuracy and increase the interpretation [7, 8].

Metal artefact reduction (MAR) algorithms [9, 10] have been developed with the purpose of reducing beam hardening-related effects and improve CBCT image quality. The Picasso Trio (Vatech, Hwaseong, Republic of Korea), ProMax 3D (Planmeca, Helsinki, Finland) and Cranex 3D (Soredex, Tuusula, Finland) are some of the CBCT units that make available MAR algorithm. Generally, this algorithm is a post-processing tool that works during image reconstruction and has no influence on image acquisition. MAR has been assessed on recent studies with regard to image quality [11,

✉ Polyane Mazucatto Queiroz
polyanequeiroz@hotmail.com

¹ Piracicaba Dental School, Department of Oral Diagnosis, Area of Oral Radiology, Piracicaba Dental School, University of Campinas, 901, Limeira Avenue, Piracicaba, Sao Paulo 13414-903, Brazil

² Department of Physiological Sciences, Area of Pharmacology, Piracicaba Dental School, University of Campinas, 901, Limeira Avenue, Piracicaba, Sao Paulo 13414-903, Brazil

12]; however, the effect of MAR algorithm on different dental materials remains unknown. Considering the great use of highly X-ray attenuating dental materials and the importance of producing CBCT images that positively contribute to the diagnostic process in clinical practice, the aim of this study was to quantitatively evaluate the in vitro efficacy of MAR algorithm on CBCT images of three dental materials.

Materials and methods

Imaging phantom preparation

Three imaging phantoms were custom-made of three cylinder-shaped dental materials (diameter, 5.4 mm; height, 5.4 mm) arranged in an isosceles triangle (base, 58 mm; height, 39 mm; Fig. 1) and surrounded by chemically activated acrylic resin (CAAR) (VIPI, Sao Paulo, Brazil). The CAAR was poured into a mould of a cylindrical polyvinyl chloride (PVC) pipe (Tigre, Sao Paulo, Brazil) of 98 mm in internal diameter and 40 mm in height with a custom-made base of acrylic resin sealing the bottom opening, with the dental material cylinders submerged 20 mm above the lower edge of the imaging phantom. To avoid air bubble formation, the imaging phantom was kept in thermal polymerisation for 1 h at 4 bar of pressure.

All three imaging phantoms had the three cylinders made of the same dental material: dental amalgam alloy Permite (South Dental Industries, Bayswater, Australia), gutta-percha (Dentsply, York, USA) or aluminium-copper (Al-Cu) alloy Duracast MS (Dental Gaucho Marquart & Cia, Barueri, Brazil). The physical density of each cylinder was calculated based on Archimedes' principle by using the analytical balance Discovery (Ohaus Corporation, Parsippany, USA) [13], and the outcomes for dental amalgam alloy, Al-Cu alloy and gutta-percha were, respectively, 10.6, 7.7 and 2.6 g/mL.

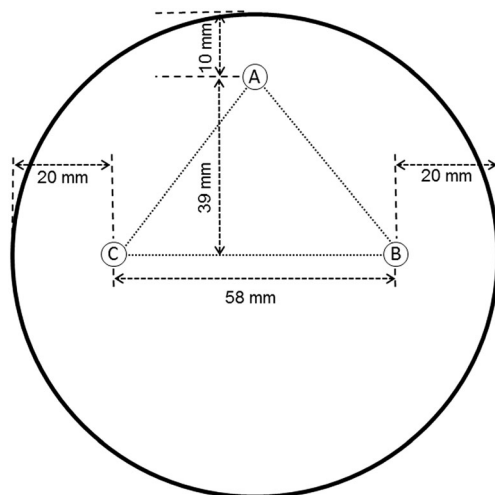


Fig. 1 Schematic drawing of an isosceles triangle used as reference for positioning the cylinders on the vertices

CBCT scanning

CBCT scans were performed by using the Picasso Trio CBCT unit (Vatech, Hwaseong, Republic of Korea) at 80 kVp, 3.7 mA, scanning time of 24 s and voxel size of 0.2 mm, and with each imaging phantom centred on an 80 × 80 mm field-of-view. All scans were repeated with the use of MAR algorithm. Volumetric data were reconstructed in the native Ez3D (E-WOO Technology, Seoul, Republic of Korea) and exported to DICOM file format.

Image analysis

A single examiner assessed all CBCT scans in OnDemand3D software (CyberMed, Seoul, Republic of Korea; Fig. 2). On axial reconstructions, six circular regions of interest (ROIs; diameter, 5.4 mm) were selected around the middle height of the three cylinders comprising a total of 18 ROIs. To determine the ROIs, the examiner selected the perimeter of the circular-shaped sample (diameter of 5.4 mm) and drew a

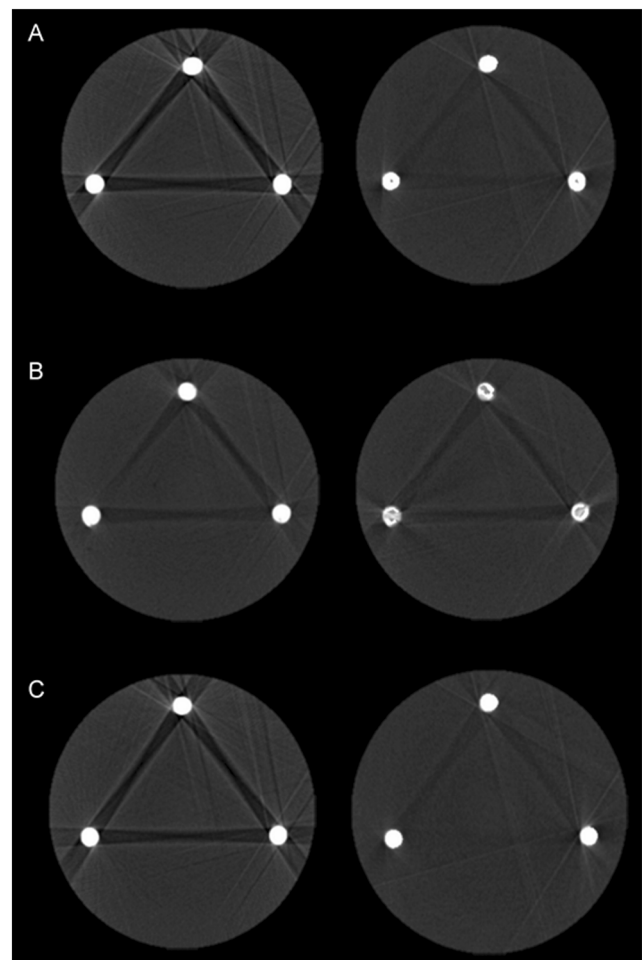


Fig. 2 CBCT axial reconstructions of imaging phantoms made of **a** dental amalgam alloy, **b** gutta-percha and **c** Al-Cu alloy. Images on the left and right sides are without and with MAR, respectively

vertical line across its centre. This line served as a reference to symmetrically arrange the upper and lower ROIs. Then, the remaining four ROIs were placed such that they were tangent to the circular sample area and to each other, as shown in Fig. 3. The same ROIs were selected in an area under no effect of the cylinder-related image artefacts (control area), 5.4 mm below the lower edge of the cylinders. Standard deviation (SD) of grey values was obtained from the ROIs around the samples as a measure of artefact expression (grey value variability). Importantly, higher SD of grey values represents greater artefact expression and worse image quality. After 90 days, 50% of the images were reevaluated to assess the reproducibility of the method.

Statistical analysis

Data distribution and variances homoscedasticity were evaluated by Kolmogorov and Smirnov and Bartlett tests, respectively. Kruskal-Wallis and Student-Newman-Keuls (post hoc) tests assessed the effect of the MAR algorithm on artefact expression from the ROIs around the dental materials and the control areas at a level of significance of 5%. The intraclass correlation coefficient (ICC) assessed the intraobserver reproducibility. All the statistical analyses were

carried out using the GraphPad Prism 6.0 (GraphPad Software, La Jolla, CA, USA) and BioEstat 5.0 (Fundação Mamirauá, Belém, PA, Brazil).

Results

The effect of MAR on artefact expression obtained for each dental material is shown in Fig. 4. Significant differences were observed between material and control ROIs irrespective of MAR. Control ROIs with MAR and without MAR (w/oMAR) did not differ among dental amalgam alloy ($p = 0.9429$), gutta-percha ($p = 0.6215$) and Al-Cu alloy ($p = 0.0883$). MAR also did not affect the material ROI of gutta-percha ($p = 0.9873$). However, MAR significantly reduced the material ROI of both dental amalgam alloy ($p = 0.0098$) and Al-Cu alloy ($p = 0.0100$). Comparisons among dental material ROIs showed no significant differences between dental amalgam and Al-Cu alloys for both MAR ($p = 0.9195$) and w/oMAR ($p = 0.2526$) conditions. In addition, both alloy ROIs of MAR and w/oMAR significantly differed ($p < 0.05$) from gutta-percha. Intraclass correlation coefficient showed excellent reproducibility with an ICC value of 0.997.

Fig. 3 Partial CBCT axial image with six circular ROIs located around a sample of dental material (Al-Cu alloy)

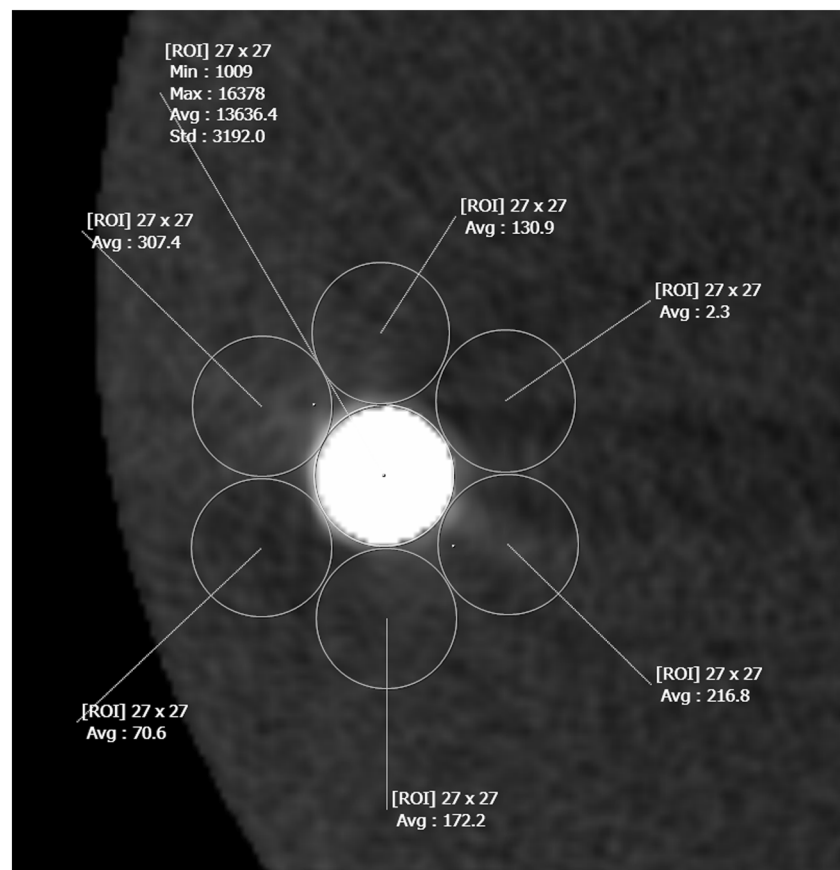
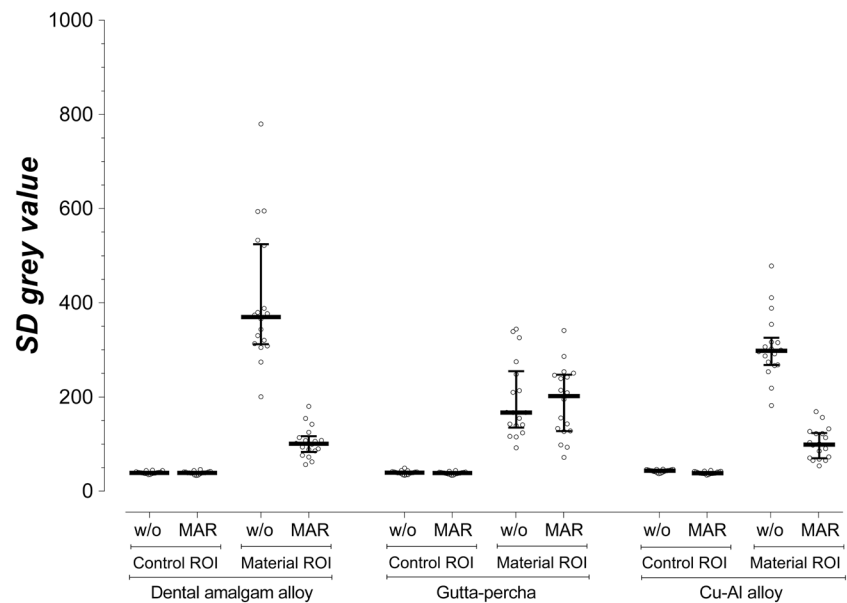


Fig. 4 Standard deviation grey values obtained without MAR (w/o) and with MAR from ROIs of the control area (control ROI) and around the dental materials (material ROI) of the imaging phantoms composed of dental amalgam alloy, gutta-percha and Al-Cu alloy. *Central bar* = median; *whiskers* = first and third quartiles



Discussion

In clinical practice, dental materials of high physical density and atomic number are commonly observed and induce the occurrence of CBCT artefact. Artefact is a clinically undesirable phenomenon that can degrade the image quality and compromise the diagnostic process.

CBCT manufactures have focused on the reduction of artefact with the development of new image data processing methods and MAR algorithms [9–12]. In the present study, MAR showed a positive influence only on CBCT images of dental alloys with a significant reduction of artefact expression. This represents a reduction of grey value variability and greater homogeneity of the image [14], which suggests a real metal artefact reduction. The fact that MAR did not reduce artefact expression in the presence of gutta-percha could be explained because this material did not produce enough image artefact to be significantly reduced by MAR. The atomic number of the main components of dental amalgam alloy are 47 (silver) and 80 (mercury) and Al-Cu alloy are 29 (copper) and 13 (aluminium), while gutta-percha is composed of a portion of zinc oxide (atomic number of zinc is 30) and isoprene rubber with a very low atomic number. Additionally, the physical densities of the cylinders used in this study were 10.6, 7.7 and 2.6 g/mL for dental amalgam alloy, Al-Cu alloy and gutta-percha, respectively. Different types of MAR algorithms should be developed to reduce artefact expression even when intermediate density materials of high atomic number are present, considering that image artefact arising from gutta-percha has shown to reduce the diagnostic accuracy of CBCT in the detection of dental root fractures [8]. Importantly, manufactures disclose limited information on the operation of algorithms.

Bechara et al. [11], Bechara et al. [12] and Bezerra et al. [6] have found similar results when assessing MAR in the

presence of a metallic sphere within the imaging phantom. However, the assessment was restricted to a single area adjacent to the sphere whose composition was not revealed. Considering the clinical importance of evaluating the entire area adjacent to the artefact source because CBCT image degradation can extend in all directions, the present study had six ROIs around the object of study.

The application of MAR algorithm on CBCT scans leads to an increase in the reconstruction time. According to the instruction manual provided by Vatech, the manufacturer of Picasso Trio CBCT unit, the extra time can be twice as long when MAR algorithm is activated. It is important to highlight that, in this particular CBCT unit, the MAR algorithm has to be selected prior to image acquisition at no specific level. Therefore, when dense materials of high atomic number are in the field-of-view, the use of MAR algorithm should be indicated to improve image quality.

Scientific studies that evaluate MAR on CBCT images of different dental materials are scarce in the literature. The evaluation of the isolated effect of MAR on CBCT scans of dental amalgam alloy, gutta-percha and Al-Cu alloy was only possible, in the present study, because many interfering factors were controlled in vitro. Caution should be used when extrapolating the results of a laboratory study on CBCT grey values to a clinical situation because each patient interacts differently with the X-ray beam.

Conclusion

MAR should be used on CBCT scans of objects containing dental amalgam and Al-Cu alloys due to its efficacy in reducing image artefact. Conversely, MAR is not recommended in the presence of gutta-percha, because this would represent an

increase in the reconstruction time without improving the image quality.

Compliance with ethical standards

Conflict of interest The authors declare that they have no conflict of interest.

Funding This work was financially supported by the Coordination for the Improvement of Higher Education Personnel, Brazil.

Ethical approval This article does not contain any studies with human or animal subjects performed by any of the authors.

Informed consent For this type of study, informed consent is not applicable.

References

1. Scarfe WC, Farman AG, Sukovic P (2006) Clinical applications of cone-beam computed tomography in dental practice. *J Cant Dent Assoc* 72:75–80
2. Bechara B, McMahan A, Moore WS, Noujeim M, Geha H (2012a) Contrast-to-noise ratio with different large volumes in a cone-beam computerized tomography machine: an in vitro study. *Oral Surg Oral Med Oral Pathol Oral Radiol* 114:658–665
3. Oliveira ML, Freitas DQ, Ambrosano GM, Haiter-Neto F (2014) Influence of exposure factors on the variability of CBCT voxel values: a phantom study. *Dentomaxillofac Radiol* 43:20140128
4. Schulze R, Heil U, Groß D, Bruellmann DD, Dranischnikow E, Schwanecke U, Schoemer E (2011) Artefacts in CBCT: a review. *Dentomaxillofac Radiol* 40:265–273
5. Gamba TO, Oliveira ML, Flores IL, Cruz AD, Almeida SM, Haiter-Neto F, Lopes SL (2014) Influence of cone-beam computed tomography image artifacts on the determination of dental arch measurements. *Angle Orthod* 84:274–278
6. Bezerra ISQ, Neves FS, Vasconcelos TV, Ambrosano GMB, Freitas DQ (2015) Influence of the artefact reduction algorithm of Picasso Trio CBCT system on the diagnosis of vertical root fractures in teeth with metal posts. *Dentomaxillofac Radiol* 44:20140428
7. Barrett JF, Keat N (2004) Artifacts in CT: recognition and avoidance. *Radiographics* 24:1679–1691
8. Neves FS, Freitas DQ, Campos PS, Ekestubbe A, Lofthag-Hansen S (2014) Evaluation of cone-beam computed tomography in the diagnosis of vertical root fractures: the influence of imaging modes and root canal materials. *J Endod* 40:1530–1536
9. Mahnken AH, Raupach R, Wildberger JE, Jung B, Heussen N, Flohr TC, Günther RW, Schaller S (2003) New algorithm for metal artifact reduction in computed tomography: in vitro and in vivo evaluation after total hip replacement. *Investig Radiol* 38:769–775
10. Maltz JS, Gangadharan B, Bose S, Hristov DH, Faddegon BA, Paidi A, Bani-Hashemi AR (2008) Algorithm for X-ray scatter, beam-hardening, and beam profile correction in diagnostic (kilovoltage) and treatment (megavoltage) cone beam CT. *IEEE Trans Med Imaging* 27:1791–1810
11. Bechara B, Moore WS, McMahan CA, Noujeim M (2012b) Metal artefact reduction with cone beam CT: an in vitro study. *Dentomaxillofac Radiol* 41:248–253
12. Bechara B, McMahan CA, Geha H, Noujeim M (2012c) Evaluation of a cone beam CT artefact reduction algorithm. *Dentomaxillofac Radiol* 41:422–428
13. Pick B, Pelka M, Beli R, Braga RR, Lohbaue U (2011) Tailoring of physical properties in highly filled experimental nanohybrid resin composites. *Dent Mater* 27:664–669
14. Webber RL, Tzukert A, Ruttimann U (1989) The effects of beam hardening on digital subtraction radiograph. *J Periodontal Res* 24:53